Research Square

Preprints are preliminary reports that have not undergone peer review.
They should not be considered conclusive, used to inform clinical practice,
or referenced by the media as validated information.

Removal of Iron and Aluminium from Reactor Storage Pool Water Using Polymer Membranes

Kryštof Konečný
Czech Technical University in Prague
Pavel Kůs
Research Centre Rez
Kateřina Čubová
katerina.cubova@fjfi.cvut.cz

Czech Technical University in Prague

Research Article

Keywords: Membrane filtration, polymer membranes, iron, aluminium

Posted Date: July 9th, 2026

DOI: https://doi.org/10.21203/rs.3.rs-10178505/v1

License: This work is licensed under a Creative Commons Attribution 4.0 International License.
Read Full License

Additional Declarations: No competing interests reported.

Title page

Names of the authors: Kryštof Konečný[1,2], Pavel Kůs[2], Kateřina Čubová[1]

Title: Removal of Iron and Aluminium from Reactor Storage Pool Water Using Polymer Membranes

Affiliation(s) and address(es) of the author(s): [1]Czech technical University in Prague, Department of Nuclear Chemistry, Břehová 7, 115 19 Prague 1, Czech Republic

[2]Research Centre Řež, Hlavní 130, Řež, 250 68 Czech Republic

E-mail address of the corresponding author: katerina.cubova@fjfi.cvut.cz

Removal of Iron and Aluminium from Reactor Storage Pool Water Using Polymer Membranes

Kryštof Konečný[1,2], Pavel Kůs[2], Kateřina Čubová[1]

[1]*Czech technical University in Prague, Department of Nuclear Chemistry, Břehová 7, 115 19 Prague 1, Czech Republic*

[2] *Research Centre Řež, Hlavní 130, Řež, 250 68 Czech Republic*

Abstract

The Research Centre Řež operates the LVR-15 reactor, where storage pool B is used for long-term storage of irradiated materials, mainly aluminium and steel. Corrosion of these materials leads to elevated concentrations of iron and aluminium in the pool water. This work investigates the use of pressure-driven membrane filtration (3.0–0.22 μm), employing two types of membranes—MCE (mixed cellulose ester) and nylon membranes—to reduce these concentrations under different pH conditions and with increased iron levels in order to evaluate colloid formation and separation efficiency.

Keywords

Membrane filtration, polymer membranes, iron, aluminium

Introduction

The Research Centre Řež operates the LVR-15 light-water research reactor with an operational thermal output of 10 MW [1], providing irradiation positions in the reflector region with neutron fluence rates of up to $5 \cdot 10^{13}$ cm^{-2} s^{-1} [2]. The reactor is used for experimental purposes and for the production of radioisotopes for medical and industrial applications. The system includes a storage pool B used for long-term storage of materials

used in irradiation (e.g., probes or irradiation channels). In most cases, this material is made of aluminium or steel.

Water in storage pool B of the LVR 15 research reactor shows persistently elevated concentrations of iron and aluminium, caused by gradual corrosion of metallic materials stored in the basin. The aim of this work was to experimentally evaluate the potential for reducing these concentrations using pressure driven membrane filtration with polymer membranes (MCE, NYL) of various pore sizes ranging from 3.0 to 0.22 μm. Filtration was tested at three pH values (acidic, neutral, alkaline) and under conditions of artificially increased iron concentration to verify the formation of colloidal particles and their potential for more efficient separation.

Membrane technologies are modern separation processes that use semipermeable membranes to separate individual components based on their size, shape, or electrical charge, usually under the influence of a pressure gradient. These technologies are widely applied in many industrial fields, such as water treatment, wastewater purification, and the food industry. The main types of membrane processes include microfiltration, ultrafiltration, nanofiltration, and reverse osmosis [3].

The experiment employed both microfiltration and ultrafiltration techniques. Microfiltration uses membranes with pore sizes typically ranging from 0.05 to 10 μm [3], enabling efficient separation of suspensions and dispersions. The process operates at relatively low pressure differences, usually up to 0.1 MPa [4]. Microfiltration can be performed either in dead-end mode, where the feed flows perpendicular to the membrane surface and retained particles accumulate on the membrane, or in cross-flow mode, where the feed flows parallel to the membrane surface, reducing particle deposition [5]. Microfiltration is widely used in water treatment, milk processing, and pharmaceuticals industry [6].

Ultrafiltration employs membranes with smaller pore sizes, typically ranging from 10 nm to 0.1 μm [7]. Compared to microfiltration, ultrafiltration operates at higher pressure differences, usually between 0.2 and 1.4 MPa [4]. Industrial applications of ultrafiltration include the concentration and purification of dairy products, clarification of fruit juices[8].

Storage pool B has a total volume of 31.68 m³ and is filled with demineralized water with a conductivity below 10 µS/cm and a TOC value below 0.2 mg/L [9]. Structurally, the pool is lined with steel and fully surrounded by heavy concrete, including the bottom section. The water in storage pool B is required to meet a set of operational limit parameters, which are summarized in Table 1.

Table 1. Operational parameters of storage pool B.

Parameter	**Value**
Specific conductivity	<10 µS/cm
pH	5,5-6,5
Chloride ion content	<0,1 mg/l
Fe	<1 mg/l

For the purposes of this work, the evaluation focused on the period from 2 January 2025 to 1 September 2025, during which samples were collected at two-week intervals, with daily sampling performed during the final five days. The concentration of CO_2 was not determined, as the pool is open to the atmosphere and the dissolved CO_2 is assumed to be in equilibrium with ambient air. All average values obtained during this period are summarized in Table 2

Table 2.Measured average values of the water in storage pool B

Parameter	**Value**
Specific conductivity	4,53 µS/cm
pH	5,90

Chloride ion content	2 µg/l
Fe	0,99 mg/l
Al	5050 µg/l
Cu	7 µg/l

In addition, the release of radionuclides from the stored materials was monitored. These measurements were carried out from 5 January 2023 to 6 November 2025 at two-week intervals, and the resulting average values showed that the dominant contributor to the activity was ^{60}Co with an activity of 334.35 Bq/L. Other detected radionuclides — including ^{95}Nb, ^{134}Cs, ^{137}Cs, ^{54}Mn, ^{59}Fe, ^{65}Zn, ^{124}Sb, and ^{51}Cr — contributed only minor activities. The total activity reached 382.88 Bq/L.

A comparison of Table 1 and Table 2 shows that the operational limits of storage pool B are not met for iron and aluminium concentration. The fact that the limits are not met is most likely related to the fact that both elements occur in a range of chemical forms, including poorly soluble oxy-hydroxide species. Filtration through the mixed-bed ion-exchange resin Amberlite MB20, consisting of a cation- and anion-exchange resin in an approximately 1:1 ratio [10], is therefore not fully effective. These oxy-hydroxide species tend to form low-solubility particles or colloids that are not efficiently captured by ion-exchange resins designed primarily for the removal of dissolved ionic species.

To better understand the behaviour of iron and aluminium in the system, speciation diagrams were constructed (Fig.1). In these diagrams, the aqueous solution was equilibrated with gaseous CO_2 at 25 °C, and the relative abundance of individual species was evaluated. Based on these diagrams, we can infer which forms the elements would adopt if they were present in the solution independently. For example, at the natural pH of 5.9, iron would be expected to occur predominantly as Fe^{2+}, whereas aluminium would be present as a mixture of Al^{3+}, $AlOH^{2+}$, $Al(OH)_2^+$, $Al(OH)_3$, and $Al(OH)_4^-$.

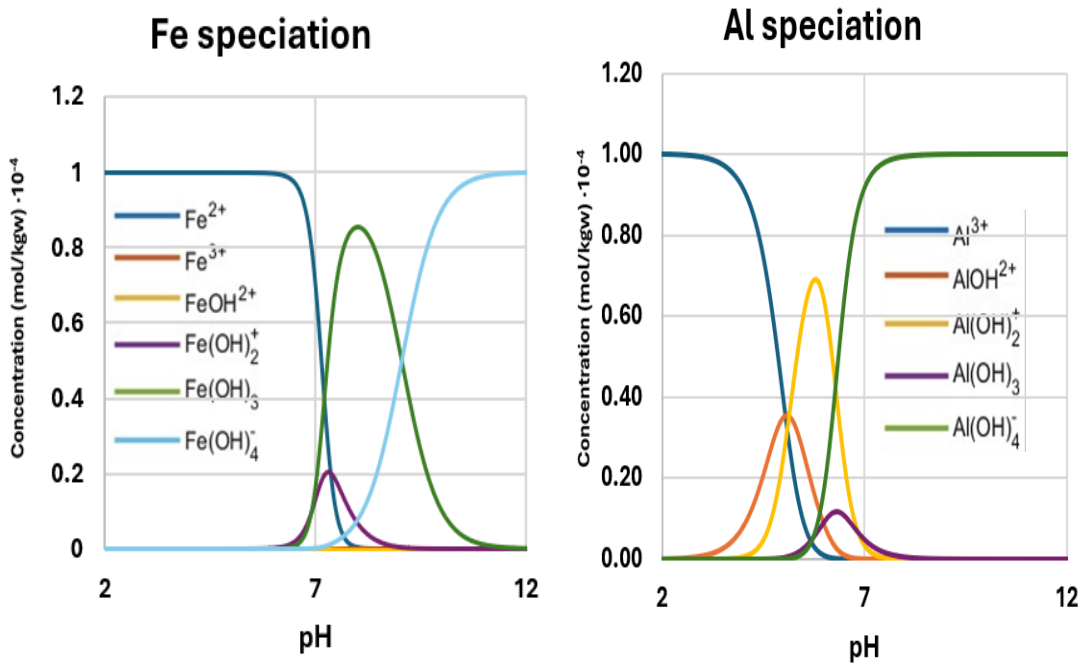


Figure1.Speciation diagram of iron and aluminium at 25 °C

Experimental

Chemicals and materials

Concentrated sulfuric acid (96 %, Chemicals Unlimited) and a certified iron stock solution with a concentration of 100.0 ± 0.2 mg/L in 5 % HCl (purity 99.998 %, ANALYTIKA spol. s r.o.) were used as received. Glacial acetic acid (p.a., Chemicals Unlimited), hydroxylamine hydrochloride (p.a., Lach-Ner, s.r.o.), ammonium acetate (p.a., Chemicals Unlimited), and 1,10-phenanthroline monohydrate (p.a., VWR Chemicals BDH) were also employed without further purification. All chemicals were of analytical grade and used as supplied. Most of the membranes were supplied by filtraTECH, except for the MCE membranes with pore sizes of 3.0 and 0.8 µm, which were manufactured by Sartorius. MCE membranes are hydrophilic polymer membranes made from cellulose nitrate and cellulose acetate, characterized by high flow rates and good mechanical stability [11]. They are generally usable within a pH range of approximately 3.5–8, beyond which chemical degradation may occur [12]. Nylon membranes are hydrophilic polyamide membranes

with good mechanical resistance and flexibility[13]. They are generally usable within a pH range of 6–13 [14].

Methods

Filtration

Water samples were collected from storage pool B and processed by membrane filtration. Filtration was carried out using mixed-cellulose-ester (MCE) membranes with nominal pore sizes 3.0, 1.2, 0.8, 0.45, and 0.22 µm, and nylon membranes with pore sizes 1.0, 0.45, and 0.22 µm. For each filtration run, 500 mL of the water sample was passed through the selected membrane using a standard vacuum filtration setup. Filtration experiments were performed both at the native pH of the water sample (pH 5.77) and under controlled pH conditions, where the pH was adjusted to 2.70 or 11.28 prior to filtration using solutions of HCl or NaOH. The concentration and volume of the acid or base were selected individually for each experiment, as the required amount depended on the initial composition of the water sample. Additional experiments were conducted with iron added to the sample at a concentration of 5 mg/L, followed by filtration under the same conditions.

From the resulting filtrate, defined sample fractions were collected for subsequent analyses. A 100 mL fraction was reserved for iron determination and immediately stabilized by adding 1 mL of concentrated H_2SO_4 (96 %). A 50 mL fraction was taken for aluminium determination. For the measurement of pH, electrical conductivity, and turbidity, a combined 100 mL fraction was collected.

Analysis

Water samples from storage pool B with pH values ranging from 2 to 12 were prepared, with individual pH values adjusted to an accuracy of ±0.5. The initial sample, with a volume of 200 mL, had an unadjusted pH of 5.87. Lower pH values were obtained by adding hydrochloric acid of various concentrations, while higher pH values were adjusted using sodium hydroxide solutions of different concentrations. In this way, samples with

the following pH values were prepared: 2.44, 3.28, 3.98, 4.61, 5.87, 7.19, 8.22, 8.77, 9.76, 10.71, and 11.61.

Measurements were performed using a Jenway 6850 spectrophotometer. For the initial measurements, a cuvette with an optical path length of 5 mm was used, and spectra were recorded in the wavelength range of 190–1100 nm with a step size of 5 nm.

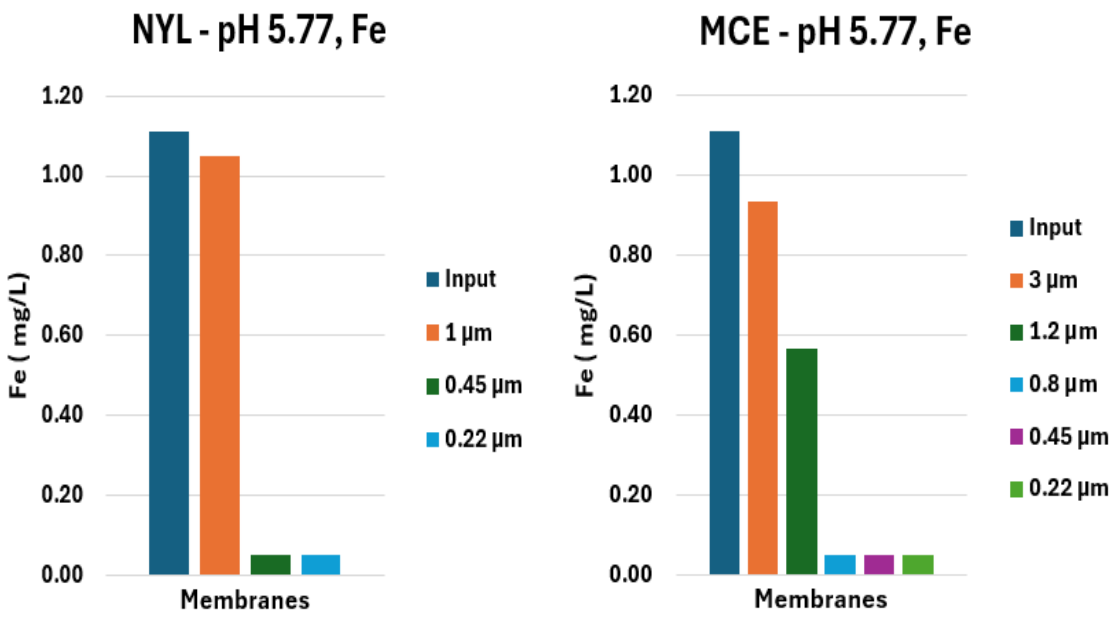
The concentration of iron in the sample fraction was determined spectrophotometrically using a Jenway 6850 UV–Vis spectrophotometer. Aluminium concentrations were measured by atomic absorption spectroscopy. The membrane filters obtained after each filtration run were subsequently analyzed by FTIR and Raman spectroscopy to characterize the retained material. The pH of the filtrate was measured using a WTW InoLab PH7310 pH meter, electrical conductivity was determined with a WTW LF 320 conductometer, and turbidity was measured using a WTW turbidimeter.

Results and discussion

Filtration

Native pH

The first set of experiments was carried out at the natural pH of the water sample with pH 5.77. Based on the measured concentrations, iron removal (Fig.2) became effective at pore sizes of approximately 0.8 µm for the MCE membranes, whereas for the nylon membranes complete retention was achieved at 0.45 µm, where the iron concentration fell below the detection limit of 0.05 mg/L. This detection limit corresponds to 4.5 % of the initial iron concentration.



159

160 *Figure 2. Concentration of Iron for NYL and MCE membranes pH 5.77*

161 A similar trend was observed for aluminium (Fig. 3); however, in this case complete
162 filtration with MCE membranes occurred only at a larger pore size of 1.2 µm. The values
163 around 0.3 mg/L shown in the graphs represent the minimum quantifiable concentration of
164 the analytical method, meaning that the actual aluminium concentrations after filtration are
165 likely even lower. This detection limit corresponds to 12.5 % of the initial aluminium
166 concentration.

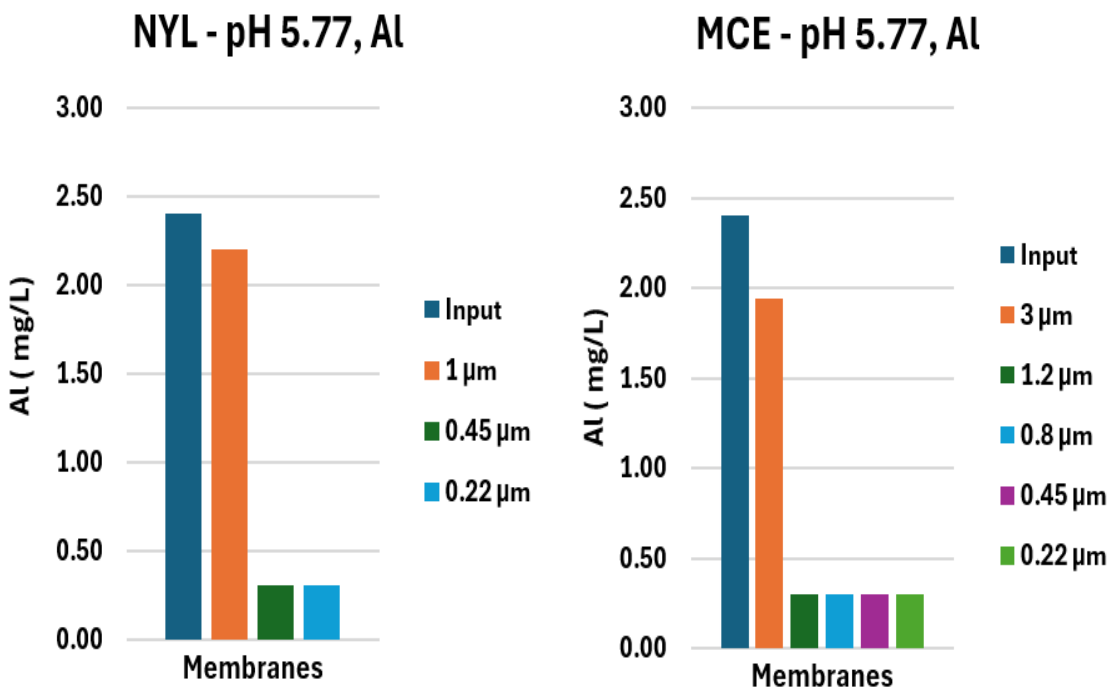
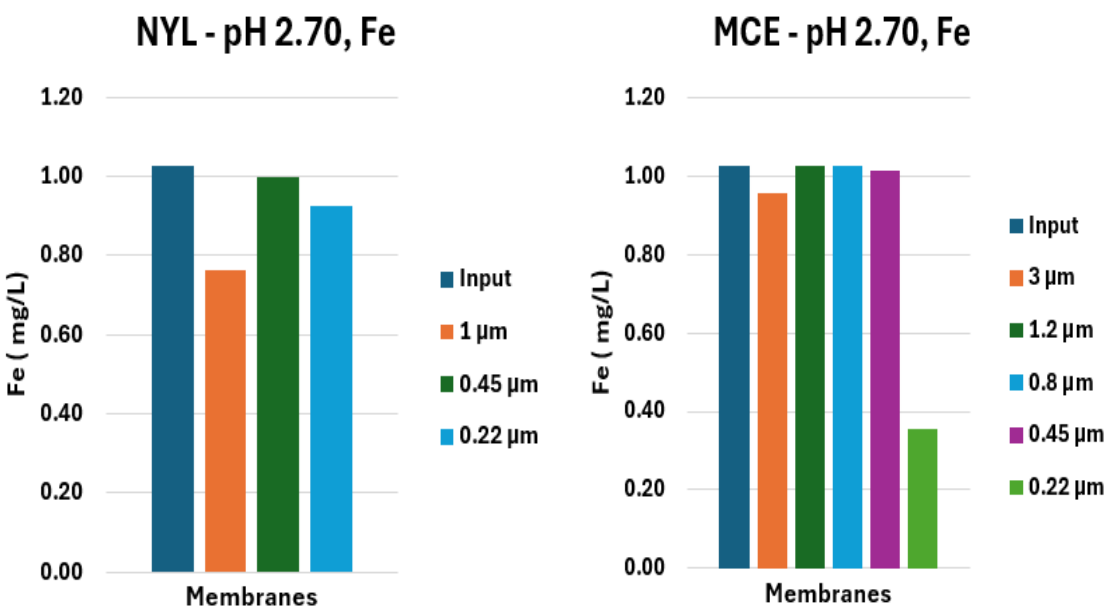


Figure 3. Concentration of Aluminium for NYL and MCE membranes pH 5.77

Acidic pH

The second set of experiments was performed at pH 2.70, which was achieved by adjusting the sample with hydrochloric acid. Under these strongly acidic conditions, the filtration performance of both MCE and nylon membranes decreased markedly. The measured concentrations show that none of the tested membranes achieved complete removal of either iron (Fig. 4) or aluminium (Fig.5). A partial exception was observed for the MCE membrane with a pore size of 0.22 µm, which exhibited the highest retention; however, even in this case the required concentration limits were not reached. For iron we achieved 33.9% of initial concentrations and for aluminium we achieved 22% of initial concentrations.

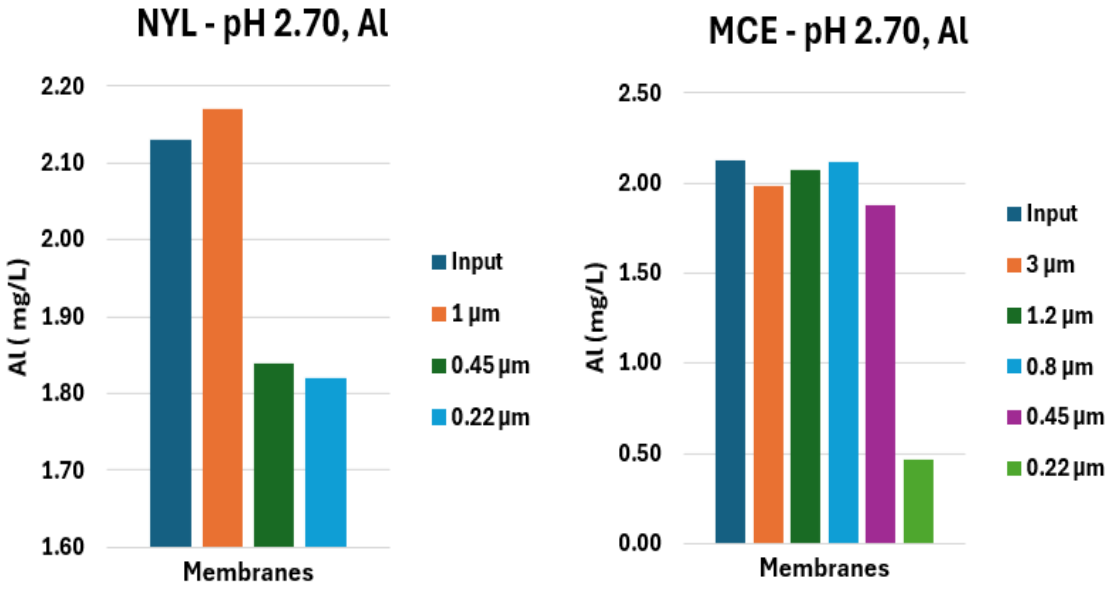
The reduced filtration efficiency at pH 2.70 is most likely related to the prevailing ionic forms of the metals. At this acidity, iron is expected to be present predominantly as Fe^{2+}, while aluminium occurs mainly as Al^{3+}. Both species are fully soluble cations, which are not retained by size-exclusion mechanisms of microfiltration membranes. This explains why even the smallest pore sizes did not provide sufficient removal under these conditions.



184

185 *Figure 4. Concentration of Iron for NYL and MCE membranes pH 2.70*

186



187

188 *Figure 5. Concentration of Aluminium for NYL and MCE membranes pH 2.70*

189 Raman spectroscopy and FTIR (Fig. 6) analysis were performed on these filters to identify
190 the solid phases retained during filtration. The spectral data indicate that the dominant
191 phases present in the samples are various forms of FeOOH, accompanied by a minor

fraction of iron oxides, specifically Fe_2O_3 and Fe_3O_4. The characteristic spectral region of these oxyhydroxides is 1000–200 cm^{-1}.

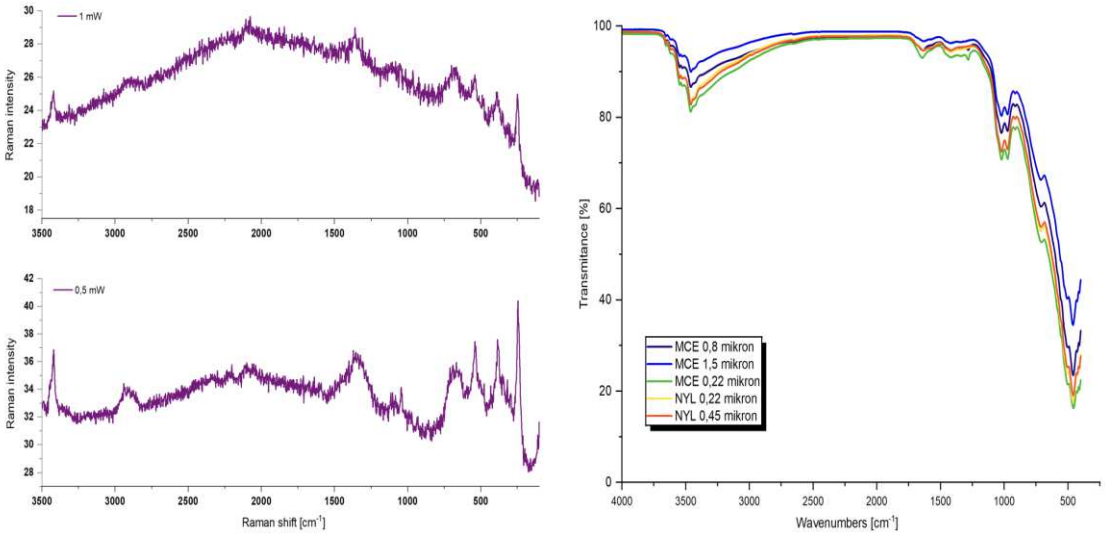


Figure 6. Raman microspectroscopy at laser power of 1 mW and 0.5 mW and FTIR

Alkaline pH

Third set of experiments was conducted at pH 11.28, which was adjusted using sodium hydroxide. Iron concentration (Fig. 7) for the MCE decreased to 23.9 % at a pore size of 0.45 µm and further to 4.49 % at 0.22 µm. Even higher removal efficiencies were achieved with the nylon membranes, where the residual iron concentration reached 4.49 % for 0.45 and 0.22 µm.

In contrast, aluminium removal (Fig. 8) was ineffective for all membrane types at pH 11.28. The measured concentrations remained close to the initial values, indicating that aluminium was present predominantly in soluble hydroxide complexes that were not retained by microfiltration membranes.

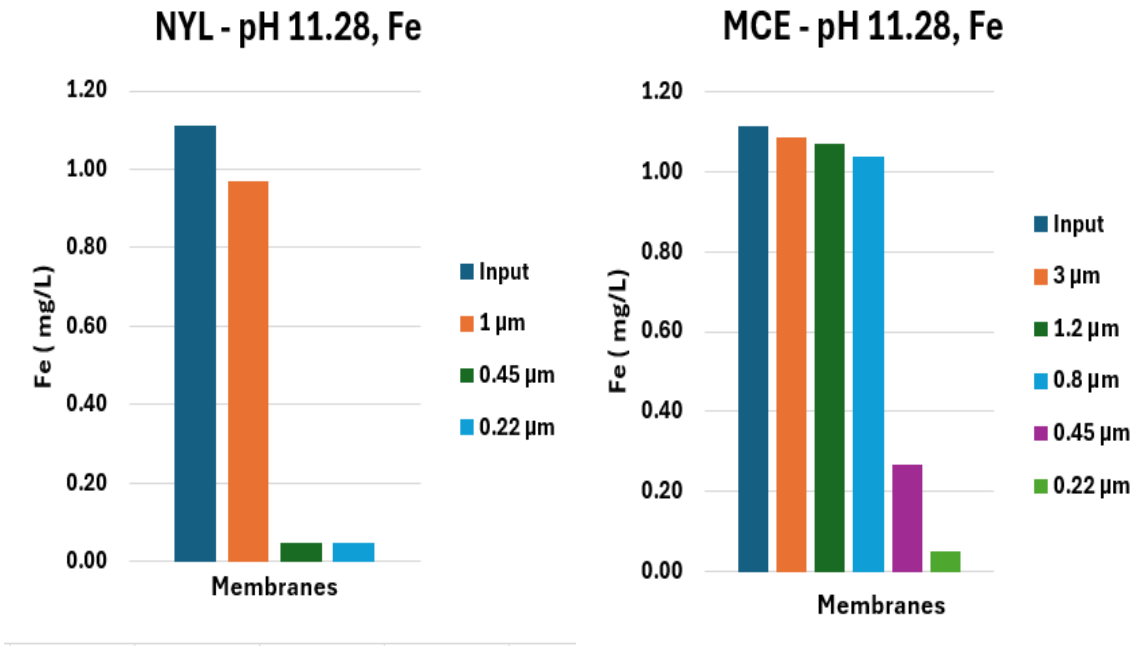


Figure 7. Concentration of Iron for NYL and MCE membranes pH 11.28

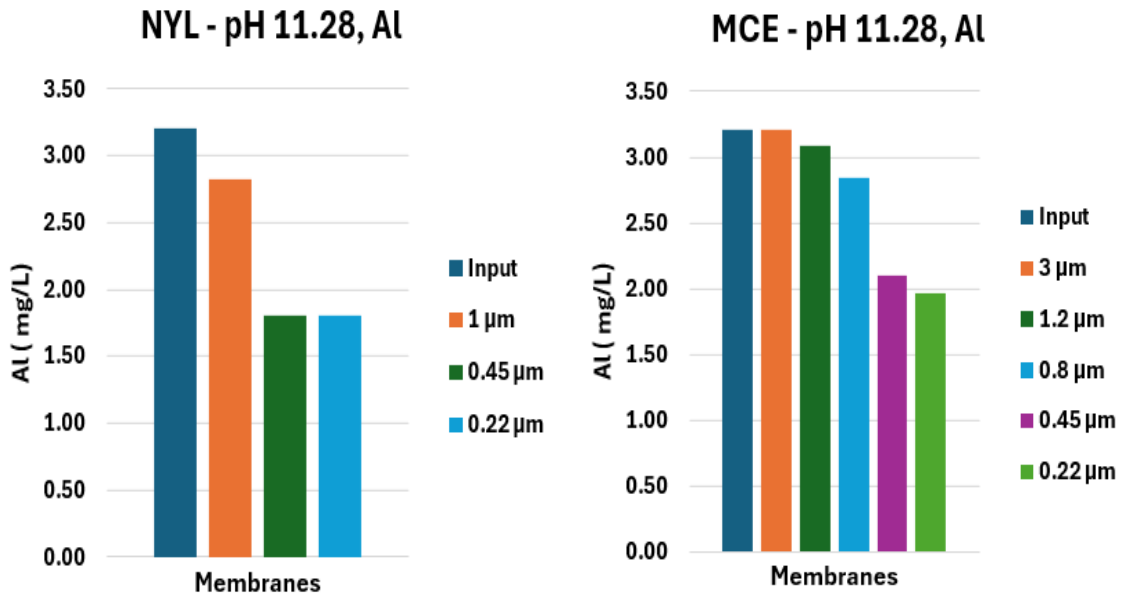
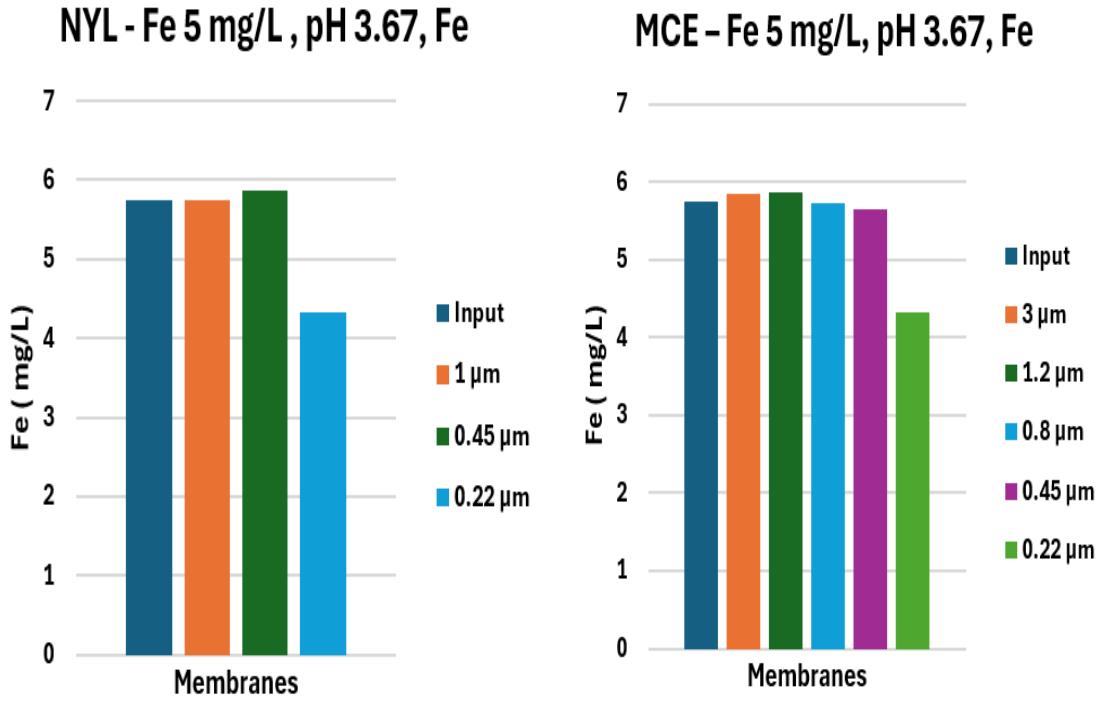


Figure 8. Concentration of Aluminium for NYL and MCE membranes pH 11.28

Iron addition

The final experiment involved the addition of 5 mg/l of iron to the water sample in an attempt to promote the formation of colloidal particles that could enhance membrane retention. However, the measured concentrations show that iron removal remained very limited (Fig. 9), and the overall filtration efficiency for iron increased only marginally compared to the unmodified sample. This indicates that the added iron did not form particulate or colloidal species of a size that would be effectively retained by the microfiltration membranes.

In contrast, a pronounced improvement was observed for aluminium removal (Fig. 10) . Both MCE and nylon membranes with a pore size of 0.22 µm achieved substantial retention, reducing the aluminium concentration to below 11.4 % of its initial value. This suggests that the presence of added iron facilitated aluminium removal, most likely through co-precipitation or co-agglomeration mechanisms, leading to the formation of larger mixed Fe–Al particles that were efficiently captured by the smallest-pore membranes.



.

Figure 9. Concentration of Iron for NYL and MCE membranes, Addition of Fe 5 mg/L pH 3.67

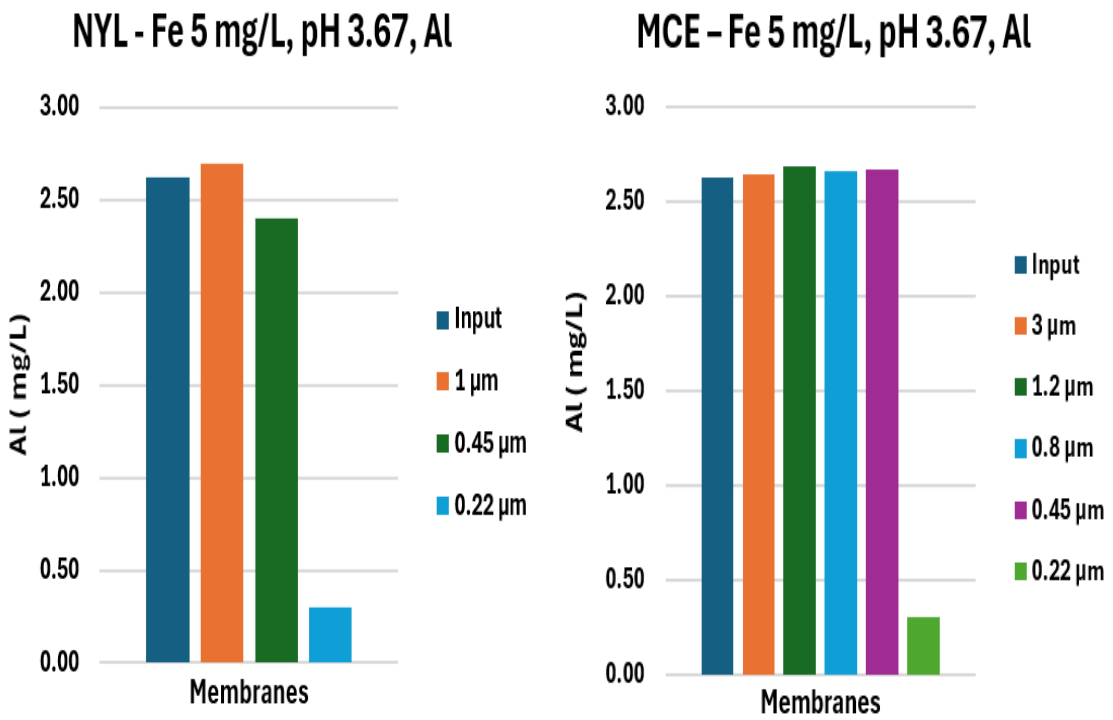


Figure 10. Concentration of Aluminium for NYL and MCE membranes, Addition of Fe 5 mg/L pH 3.67

Speciation analysis

This section presents the spectrophotometric determination of individual species as a function of pH in the range of 2–12. Based on the obtained absorption spectra, wavelengths corresponding to the maximum absorbance of each species were identified. In addition, speciation diagrams describing the distribution of individual species as a function of pH were calculated using PHREEQC. From the combination of these results, the pH interval in which filtration of the given species is expected to be most efficient was estimated.

In Figure 11 the individual samples were ordered in the legend according to their maximum absorbance values. The investigated wavelength range was limited to 190–290 nm, since at higher wavelengths no significant differences in absorbance between the samples were observed.

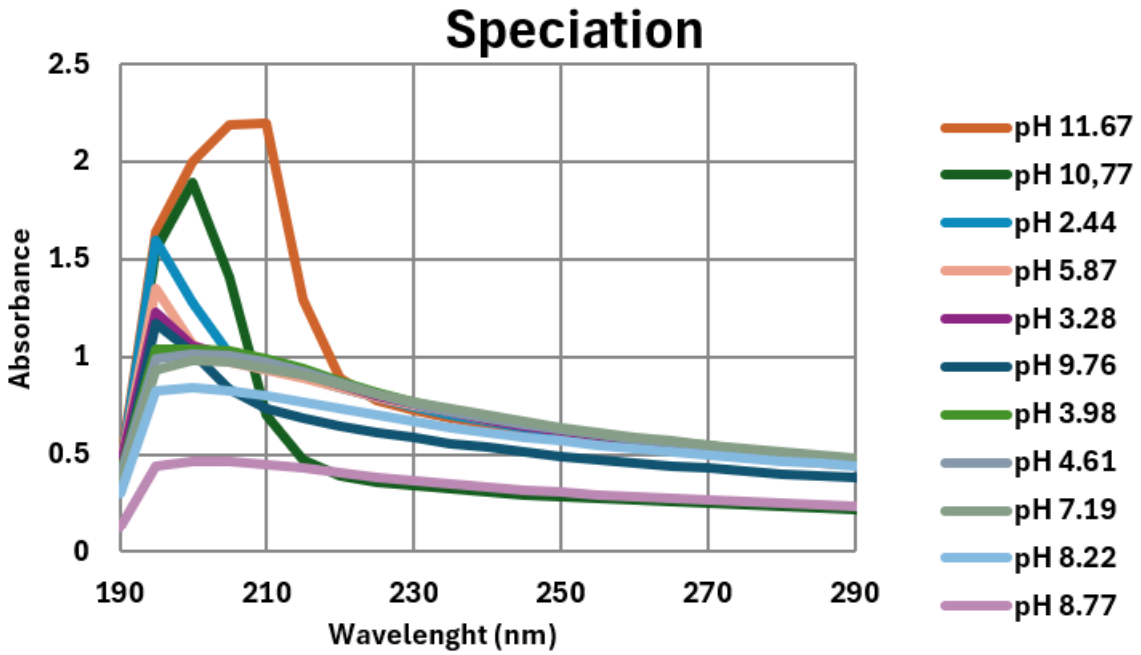


Figure 11. Absorbance of samples as a function of wavelength

Subsequently, a Table 3 was compiled containing the maximum absorbance values at the corresponding wavelengths and the predicted forms of iron and aluminium, based on the speciation diagrams (Fig. 1).

Table 3. Maximum absorbance and iron/aluminium species

pH	Max absorbance	Wavelength (nm)	Fe species	Al species
11.67	2.1984	210	$Fe(OH)_4^-$	$Al(OH)_4^-$
10.77	1.894	200	$Fe(OH)_4^-$, $Fe(OH)_3$	$Al(OH)_4^-$
9.76	1.169	195	$Fe(OH)_4^-$, $Fe(OH)_3$	$Al(OH)_4^-$
8.77	0.4623	205	$Fe(OH)_4^-$, $Fe(OH)_3$, $Fe(OH)_2^+$	$Al(OH)_4^-$

8.22	0.8413	220	$Fe(OH)_4^-$, $Fe(OH)_3$, $Fe(OH)_2^+$	$Al(OH)_4^-$
7.19	0.9786	200	$Fe(OH)_4^-$, $Fe(OH)_3$, $Fe(OH)_2^+$, Fe^{2+}	$Al(OH)_4^-$, $Al(OH)_3$, $Al(OH)_2^+$
5.87	1.3492	195	Fe^{2+}	$Al(OH)_4^-$, $Al(OH)_3$, $Al(OH)_2^+$, $AlOH^{2+}$,Al^{3+}
4.61	1.0153	200	Fe^{2+}	$Al(OH)_2^+$, $AlOH^{2+}$,Al^{3+}
3.98	1.0413	200	Fe^{2+}	$AlOH^{2+}$,Al^{3+}
3.28	1.228	195	Fe^{2+}	$AlOH^{2+}$,Al^{3+}
2.44	1.5972	195	Fe^{2+}	Al^{3+}

As shown in Table 3, the highest total number of species present for both iron and aluminium occurs at pH 7.19. However, according to Figure 11, this pH value exhibits the third-lowest absorbance. In contrast, the highest absorbance is observed at pH 11.67, where both elements occur predominantly as anion hydroxides.

Conclusions

The aim of this study was to evaluate the removal efficiency of iron and aluminium from water originating from storage pool B using microfiltration membranes of different pore sizes and to assess how filtration performance is affected by pH and metal speciation. The results clearly demonstrate that filtration efficiency is strongly dependent on the chemical conditions of the system.

At the natural pH of 5.77, both metals were removed most effectively. Membranes with pore sizes below 0.8 µm reduced iron concentrations below the detection limit of 0.05 mg/L, while aluminium concentrations also decreased substantially, indicating that a significant portion of both metals was present in particulate or colloidal forms that could be retained by microfiltration. In contrast, at pH 2.70, neither iron nor aluminium was efficiently removed, as both metals occurred predominantly as soluble ionic species that readily pass through filtration membranes. At pH 11.28, iron removal improved only for membranes with the smallest pore sizes, where precipitated hydroxide phases were effectively retained, whereas aluminium remained largely in soluble aluminate complexes and was therefore not removed.

The addition of 5 mg/L Fe was expected to promote the formation of colloidal particles and enhance filtration. However, iron removal increased only marginally, while aluminium removal improved significantly for the smallest-pore membranes, suggesting co-precipitation or co-agglomeration between Fe and Al species. Spectroscopic characterization of the retained solids was performed on filters obtained at pH 2.70 using Raman spectroscopy and FTIR analysis. The spectra confirmed the presence of FeOOH phases, accompanied by minor amounts of Fe_2O_3 and Fe_3O_4, indicating that even under strongly acidic conditions a portion of iron was present in solid hydroxide and oxide forms that were captured on the membrane surface.

Overall, the results show that pH-dependent speciation plays a dominant role in determining filtration efficiency, but the observed behaviour cannot be explained by speciation diagrams alone. Interactions between dissolved ions, colloidal particles, and membrane surfaces also significantly influence removal performance. These findings highlight the importance of considering both chemical speciation and particle-forming processes when designing or optimizing membrane-based treatment strategies for iron- and aluminium-containing waters.

Acknowledgements

The presented results were obtained using the CICRR infrastructure, which is financially supported by the Ministry of Education, Youth and Sports - project LM2023041, and by CTU grant no. SGS24/148/OHK4/3T/14.

References

[1] *Research Centre Řež – LVR-15 research reactor (n.d). https://www.cvrez.cz/cs/vyzkum-a-sluzby/provoz-reaktoru/vyzkumny-reaktor-lvr-15-12065. Accessed 22 Jan 2026*

[2] Centre for Ionising Radiation and Radiochemistry (CICRR) (n.d.) LVR-15 reactor. . https://www.cicrr.cz/lvr-15-reactor. Accessed 15 Jun 2026

[3] Palatý Z, Bernauer B (2012) Membrane Processes. University of Chemistry and Technology, Prague

[4] International Atomic Energy Agency (2004) Application of Membrane Technologies for Liquid Radioactive Waste Processing. IAEA, Vienna

[5] Abd El-Ghaffar MA, Tieama HA (2017) A Review of Membranes Classifications, Configurations, Surface Modifications, Characteristics and Its Applications in Water Purification. Chem Biomol Eng. DOI 10.11648/j.cbe.20170202.11

[6] Anis SF, Hashaikeh R, Hilal N (2019) Microfiltration membrane processes: A review of research trends over the past decade. J Water Process Eng 32:100941. DOI 10.1016/j.jwpe.2019.100941

[7] Aziz S, Mazhar AR, Ubaid A, Shah SMH, Riaz Y, Talha T, Jung DW (2024) A comprehensive review of membrane-based water filtration techniques. Applied Water Science 14:169. DOI 10.1007/s13201-024-02226-y.

[8] Shekin J (2021) Applications of ultrafiltration, reverse osmosis, nanofiltration, and microfiltration in dairy and food industry. Extsv Rev 1:39–48. DOI 10.21467/exr.1.1.4468

[9] Kůs P, Kořenková H, Klupák V, Viererbl L (2019) Monitoring of physico-chemical parameters and volume activity in tanks in storage facilities A, B and the wet storage tank. ÚJV Řež, Řež

[10] *Merck (2026) Mixed cellulose ester membrane filter. https://www.sigmaaldrich.com/CZ/cs/product/sial/428736. Accessed 14 Apr 2026*

[11] Hahnemühle Life Science (n.d) Mixed cellulose ester membranes. https://lifescience.hahnemuehle.com/en/filtration/lab-filtration/membrane-filters/mixed-cellulose-ester-membranes.html. Accessed 14 Feb 2026

[12] Hawach Scientific (n.d) MCE membrane filters. https://www.hawachmembrane.com/product/mce-membrane-filters/. Accessed 2 May 2026

[13] Cytiva Whatman (n.d) Filter papers and membranes. https://www.whatman.co.kr/pds/03.pdf. Accessed 9 Mar 2026

[14] Hawach Scientific (n.d) Nylon membrane filters. https://www.hawachmembrane.com/product/nylon-membrane-filters/. Accessed *9 Mar 2026*